INTERNATIONAL JOURNAL FOR NUMERICAL METHODS IN FLUIDS, VOL. 6, 623–639 (1986)

SOME NEW METHODS FOR NUMERICALLY SOLVING THE COMPRESSIBLE LAMINAR BOUNDARY LAYER EQUATIONS

R. G. FRIEL

Department of Computer Science, Trinity College, Dublin 2, Ireland

SUMMARY

Four new methods are presented: a method of accelerating the truncation error convergence, a fourth and fifth order difference scheme for discretizing the normal partial derivatives, high order quadrature formulae for integrating a stream function and a third order implicit scheme for treating the streamwise partial derivatives. These are seen to be effective in finding solutions to the boundary layer equations in which the step sizes are adaptively altered to meet an error bound.

INTRODUCTION

The Navier–Stokes equations describing the motion of a continuous fluid are simplified to the Eulerian equations by letting the viscosity and thermal conductivity be zero. This reduces the order of the equations from 2 to 1 and means that the actual body boundary condition of zero velocity cannot be imposed and that a slip velocity and temperature discontinuity must be permitted at the wall.

The Euler equations are obtained by letting $\mu_\infty = 0$ where μ_∞ is a characteristic viscosity of the flow. The boundary layer equations are obtained from the Navier–Stokes equations in the double limit $\mu_\infty \to 0$, $y \to 0$ where y is the co-ordinate normal to the wall. This is given in, for example, Reference 1, pp. 1–20.

The algorithm presented is able to predict the position of the separation point to within a user-defined accuracy.

Although axisymmetric boundary layers may be solved almost as easily as two-dimensional problems[2] this paper confines itself to the two-dimensional case.

One aim is to devise schemes which can find adaptive solutions to problems in which $\mathrm{d}U_e/\mathrm{d}x$ would be high near the stagnation point. U_e is the edge velocity and x is the distance from the stagnation point in a blunt body flow (see Figure 1). This implies that the equations must be solved over at least two grids, the solutions compared and the mesh sizes decreased and the problem resolved if the error limit is not met or the mesh size increased if the errors are considerably less than the required limit.

Initially the linearized Crank–Nicolson method of Cooke and Mangler[3] was used. The only innovation being the truncation error extrapolation described in section 9. The 4th and 5th order schemes described in sections 5–7 were then derived. A 3rd order scheme was also used for the streamwise derivatives as opposed to the 'smeared' schemes of Cooke and Mangler.[3] These were found to be most effective.

0271–2091/86/090623–17$08.50

Received March 1986

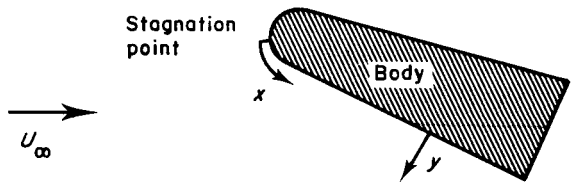

Figure 1. A sketch illustrating the co-ordinate system: x is the streamwise distance along the body and y the normal distance

2. THE PRIMITIVE EQUATIONS

The equations are first presented in their primitive form to clarify the symbols used.

The conservation equations (obtained from the Navier–Stokes equations in the limit $\mu_\infty \to 0$, $y \to 0$) are

Mass

$$\frac{\partial(\rho U)}{\partial x} + \frac{\partial(\rho V)}{\partial y} = 0 \tag{1}$$

x-momentum

$$\rho U \frac{\partial U}{\partial x} + \rho V \frac{\partial U}{\partial y} = -\frac{\partial p}{\partial x} + \frac{\partial}{\partial y}\left(\mu \frac{\partial U}{\partial y}\right) \tag{2}$$

y-momentum

$$\frac{\partial p}{\partial y} = 0 \tag{3}$$

This means that the pressure across the boundary layer has its free stream body value for that x co-ordinate.

Energy

$$\rho U \frac{\partial h}{\partial x} + \rho V \frac{\partial h}{\partial y} = U \frac{\partial p}{\partial x} + \mu\left(\frac{\partial U}{\partial y}\right)^2 - \frac{\partial q}{\partial y} \tag{4}$$

where ρ is the density, U and V the x and y velocity components, p is the pressure, h is the specific enthalpy, μ is the viscosity and q is the heat-transfer rate.

An ideal gas is used in the examples given here and its properties are as follows. An explicit state equation $h = [\gamma/(\gamma - 1)]\,(p/\rho)$ is assumed. $\gamma = c_p/c_v$ is the ratio of the constant pressure to constant volume specific heats. The viscosity μ is assumed to vary according to Sutherland's law[1] which states that

$$\mu = \text{a constant} \frac{T^{3/2}}{T + C^*} \tag{5}$$

where T is the absolute temperature and, C^* is a constant which is taken to be 117 K for air.

The Prandtl number $Pr = (\mu c_p)/\lambda$ is assumed to be constant, and a value of 0·72 has been taken for air. As the constant pressure specific heat c_p is constant for an ideal gas the thermal conductivity λ varies inversely to μ.

The heat-transfer rate q in equation (4) is given by

$$q = -\frac{\mu}{Pr}\frac{\partial h}{\partial y} \tag{6}$$

The higher order methods could be used to calculate dissociating laminar boundary layers.

3. THE PRIMITIVE BOUNDARY CONDITIONS

The equations (2) and (3) are parabolic. Using the analogy with transient one-dimensional heat conduction the x-dimension is time like and the y-axis is space like. No boundary conditions have yet been imposed. Reverting to the heat conduction analogy, the temperature profile at time $t = 0$ is given in addition to the boundary conditions at the end points for $t \geqslant 0$. This is equivalent, in this problem, to knowing the stagnation point profile at which $x = 0$. This, however, has to be calculated, and one of the reasons why the equations must be transformed is to allow this starting profile to be computed. In this section the function $f(x)$ is some, not necessarily continuous, function of the dependent variable x which is given by the user.

The boundary conditions on (1), (2) and (4) are

(i) at the wall ($y = 0$):

$$U = 0: \text{no slip condition} \tag{7}$$

$$(\rho V) = f(x) \tag{8}$$

where $f(x)$ is a function giving the wall surface mass transfer. This is taken as zero in the examples given.

On the energy equation one of (9), (10) or (11) may be imposed:

$$h = f(x) \tag{9}$$

where the function $f(x)$ specifies the wall enthalpy,

$$\left(\frac{\partial h}{\partial y}\right) = f(x) \tag{10}$$

where the function $f(x)$ specifies the wall enthalpy normal derivative, or

$$f(x) = \left(\frac{\mu}{Pr}\right)\left(\frac{\partial h}{\partial y}\right) - \sigma\varepsilon(T)T^4 \tag{11}$$

where σ is the Stefan–Boltzmann constant and $\varepsilon(T)$ is the emissivity, which is normally a weak function of T. The function $f(x)$ specifies the wall heat transfer imbalance between radiative losses and conductive gains from the boundary layer. Specifying $f(x) = 0$ for all x implies that there is, at each point on the body, local equilibrium between radiation and the heat conducted in from the boundary layer.

(ii) At the edge of the boundary layer ($y \to \infty$):

$$U \to U_e \tag{12}$$

where $U_e(x)$ is the wall slip velocity from the inviscid solution.

$$H \to H_s \tag{13}$$

where H_s is the total enthalpy (constant along the body streamline).

$$H_s = h_\infty + \frac{U_\infty^2}{2} \tag{14}$$

4. THE TRANSFORMED EQUATIONS

The equations and their boundary conditions, in their primitive form, are not amenable to being approximately solved for two reasons: first the problem of generating the starting stagnation point profiles and, secondly, the problem of the growth of the boundary layer thickness; the distance to which the boundary layer equations must be solved grows rapidly. Reverting to the heat conduction analogy the space domain would expand rapidly and unpredictably as time increased.

The transform used is originally due to Clutter and Smith[4] and has been used by Jaffe and Smith[2] and Cooke and Mangler.[3] It is used slightly differently here: Jaffe and Smith[2] use the free stream conditions as the reference point; the stagnation conditions are used here and Cooke and Mangler[3] non-dimensionalize flow variables before transforming them. This is unnecessary; the transform itself performs the non-dimensionalization (the x co-ordinate remains dimensional but appears, in the transformed equations, as a term $x\partial\chi/\partial x$, where χ is dimensionless). Thus dividing x by a characteristic length and then taking difference expressions for its first derivative in this system will be identical to leaving it in the original dimensioned form.

The transform neglects higher order transverse curvature terms but these are only relevant to axisymmetric flows. Let

$$I = \int_0^y \rho \, dy \quad \text{and} \quad \eta = \sqrt{\frac{U_e}{\rho_s \mu_s x}} I \tag{15}$$

where the equations are to be written with x and η as dependent variables. ρ_s and μ_s are the density and viscosity at the stagnation point. U_e is the (dimensioned) velocity at the edge of the boundary layer (or, equivalently, the slip velocity on the wall). Define a stream function ψ satisfying:

$$\rho U = \frac{\partial \psi}{\partial y} \quad \text{and} \quad \rho V = -\frac{\partial \psi}{\partial x} \tag{16}$$

The following relations between the partial derivative operators are used to transform the equations:

$$\begin{aligned}\left(\frac{\partial}{\partial x}\right)_y &= \left(\frac{\partial}{\partial x}\right)_\eta + \left(\frac{\partial \eta}{\partial x}\right)_y \left(\frac{\partial}{\partial \eta}\right)_x \\ &= \left(\frac{\partial}{\partial x}\right)_\eta + \left(\frac{1}{2}\frac{\eta}{U_e}\frac{dU_e}{dx} - \frac{1}{2}\frac{\eta}{x} + \eta\frac{(\partial I/\partial x)_\eta}{I}\right)\left(\frac{\partial}{\partial \eta}\right)_x\end{aligned} \tag{17}$$

and

$$\left(\frac{\partial}{\partial y}\right)_x = \left(\frac{\partial \eta}{\partial y}\right)_x \left(\frac{\partial}{\partial \eta}\right)_x = \sqrt{\frac{U_e}{\rho_s \mu_s x}} \rho \left(\frac{\partial}{\partial \eta}\right)_x \tag{18}$$

The subscript denotes a constant value of the subscripted dependent variable. A second, dimensionless, stream function ϕ is introduced, which satisfies

$$\left(\frac{\partial \phi}{\partial \eta}\right)_x = \frac{U}{U_e} = u \tag{19}$$

where u is a dimensionless velocity. The relationship between ψ and ϕ is

$$\psi = \sqrt{\rho_s \mu_s U_e x}\,\phi \tag{20}$$

The pressure in the boundary layer is given by its inviscid value; so

$$\frac{\partial p}{\partial x} = -\rho_e U_e \frac{dU_e}{dx} \tag{21}$$

The definition of ψ incorporates the mass conservation equation, and the x momentum equation becomes

$$\partial\left(C\frac{\partial^2\phi}{\partial\eta^2}\right)\Big/\partial\eta + P\left(\frac{\rho_e}{\rho} - \left(\frac{\partial\phi}{\partial\eta}\right)^2\right) + N\phi\frac{\partial^2\phi}{\partial\eta^2} = x\left(\frac{\partial\phi}{\partial\eta}\frac{\partial^2\phi}{\partial\eta\partial x} - \frac{\partial^2\phi}{\partial\eta^2}\frac{\partial\phi}{\partial x}\right) \tag{22}$$

where

$$C = \frac{\rho\mu}{\rho_s\mu_s}, \quad P = \frac{x}{U_e}\frac{dU_e}{dx} \quad \text{and} \quad N = \frac{P+1}{2} \tag{23}$$

Let

$$\phi^* = N\phi + x\frac{\partial\phi}{\partial x} \tag{24}$$

Using u as defined in (19) gives

$$\partial\left(C\frac{\partial u}{\partial\eta}\right)\Big/\partial\eta + P\left(\frac{\rho_e}{\rho} - u^2\right) + \phi^*\frac{\partial u}{\partial\eta} = xu\frac{\partial u}{\partial x} \tag{25}$$

Values of ϕ^* are found by differentiating (24) to give

$$\frac{\partial\phi^*}{\partial\eta} = Nu + x\frac{\partial u}{\partial x} \tag{26}$$

If there is no surface mass transfer at the wall then $\phi = 0$ at $\eta = 0$ and, from (24), it can be seen that $\phi^* = 0$ at the wall. Equation (26) can then be integrated to give values of ϕ^*. The energy conservation equation (4) is written with the dimensionless total enthalpy $s = H/H_s$ as the dependent variable and with η and x as independent variables to give

$$\partial\left(\frac{C}{Pr}\frac{\partial s}{\partial\eta}\right)\Big/\partial\eta + \phi^*\frac{\partial s}{\partial\eta} + \frac{U_e^2}{H_s}\left(1 - \frac{1}{Pr}\right)\partial\left(Cu\frac{\partial u}{\partial\eta}\right)\Big/\partial\eta = xu\frac{\partial s}{\partial x} \tag{27}$$

5. SOLVING THE EQUATIONS

A shooting method is used by Jaffe and Smith[2] to perform the normal co-ordinate integration of equations (22) and (27). A value of the dependent variable first derivative at the wall is assumed and the equation is approximately solved by a Runge–Kutta or multistep method. The values of these derivatives are, in the non-linear case, iteratively altered until the outer boundary condition is met.

An alternative method is to use a linearized Crank–Nicolson scheme to solve equations (25) and (27). This was originally chosen as there appeared to be a way of performing a global Richardson-style extrapolation to decrease the truncation errors. Section 9 describes the method and the difficulty encountered in finding an interpolating function which fills in the gaps left after the extrapolated solution is found at half the normal direction meshpoints. This restriction does not apply to using the method to reduce the streamwise truncation errors.

However, the main innovation in this paper is in the derivation of 4th (and 5th) order non-centred difference schemes for this problem. These schemes rely on the fact that the η co-ordinate of the edge of the boundary layer is determined by the solution of the equations. Extending the boundary layer cannot make the solution worse, and the values of the edge conditions may be extended without error.

The value of η_∞ is not known exactly. If it is made too small then the boundary layer will not be

properly solved, if it is too big there will be wasted computation. η_∞ is normally between 5 and 7 (this was also found to be the case in Reference 2).

Using high order centred Lagrange difference approximations normally poses difficulties at the boundaries. The scheme presented here does not. It only has one point nearer to the wall than the point at which the difference operator is being applied. It can therefore treat value or derivative boundary conditions at the wall as easily as a centred 2nd order scheme. At the outer edge of the boundary layer values of the dependent variables are required. Because the boundary layer edge conditions can be extended these will be *exactly* 1. It may be possible to use the non-centred scheme, in cases where this edge extendibility does not apply, by using a centred or lower order non-centred scheme near the boundary away from the rapid variation in the dependent variable, but this has not been investigated.

Because there is only one element below the diagonal in the matrix obtained when the scheme is used in a Crank–Nicolson or implicit method the effort in solving the resulting banded Hessenberg matrix is only slightly greater than that to solve a tridiagonal system. The operation counts are (where n is the dimension):

Tridigonal 2nd order scheme: $3(n-1)$ additions/subtractions, $(2n-1)$ divisions and $3(n-1)$ multiplications.

Hessenberg 4th and 5th order scheme: $9(n-1)$ additions/subtractions, $(2n-1)$ divisions and $9(n-1)$ multiplications.

6. NORMAL CO-ORDINATE DIFFERENCE SCHEME

The following difference approximations are used to replace the first and second partial derivatives with respect to η at η_i:

$$\frac{\partial f}{\partial \eta} = \frac{-12f_{i-1} - 65f_i + 120f_{i+1} - 60f_{i+2} + 20f_{i+3} - 3f_{i+4}}{60\delta\eta} + \frac{(\delta\eta)^5}{30} f_i^{(\mathrm{vi})} + \cdots \tag{28}$$

and

$$\frac{\partial^2 f}{\partial \eta^2} = \frac{10f_{i-1} - 15f_i - 4f_{i+1} + 14f_{i+2} - 6f_{i+3} + f_{i+4}}{12(\delta\eta)^2} + \frac{13(\delta\eta)^4}{180} f_i^{(\mathrm{vi})} + \cdots \tag{29}$$

When this approximation is used implicity it gives a banded Hessenberg matrix. At the outer edge of the boundary layer values for f_{i+2}, f_{i+3} and f_{i+4} are required. For both u and s these are 1. The scheme cannot be extended further: the absolute value of the diagonal element in the approximation to the second derivative becomes less than 1 and the method becomes unstable.

7. QUADRATURE FORMULAE FOR EQUATION (26)

Cooke and Mangler[3] used the following expression to find an approximate value of ϕ^* at the point $((m+\theta)\delta x, (n-\frac{1}{2})\delta\eta)$. This is basically an application of the trapezoidal rule to perform the normal integration using an averaged central difference approximation for the streamwise derivative $(\partial u)/(\partial x)$. This gives

$$\frac{\phi^*_{m+\theta,n} - \phi^*_{m+\theta,n-1}}{\delta\eta} = N((m+\theta)\delta x)\tfrac{1}{2}(\theta u_{m+1,n} + (1-\theta)u_{m,n} + \theta u_{m+1,n-1} + (1-\theta))u_{m,n-1}$$
$$+ (m+\theta)\delta x \frac{(u_{m+1,n} - u_{m,n}) + (u_{m+1,n-1} - u_{m,n-1})}{2\delta x} \tag{30}$$

Again the edge extendability allows better quadrature formulae for integrating (26) to be constructed. These are found by fitting the Lagrangian polynomial through the points f_i, f_{i+1}, $f_{i+2},\ldots,f_{i+n}$ and integrating it and then finding the value of this definite integral between η_i and η_{i+1}. This is analogous to the construction of a corrector formula in a multistep method. The 3 point formula is

$$\int_{\eta_i}^{\eta_i+\delta\eta} f\,\mathrm{d}\eta = \delta\eta\frac{5f_i+8f_{i+1}-f_{i+2}}{12}+E[f] \tag{31}$$

4 point:

$$\int_{\eta_i}^{\eta_i+\delta\eta} f\,\mathrm{d}\eta = \delta\eta\frac{9f_i+19f_{i+1}-5f_{i+2}+f_{i+3}}{24}+E[f] \tag{32}$$

5 point:

$$\int_{\eta_i}^{\eta_i+\delta\eta} f\,\mathrm{d}\eta = \delta\eta\frac{251f_i+646f_{i+1}-264f_{i+2}+106f_{i+3}-19f_{i+4}}{720}+E[f] \tag{33}$$

6 point:

$$\int_{\eta_i}^{\eta_i+\delta\eta} f\,\mathrm{d}\eta = \delta\eta\frac{475f_i+1427f_{i+1}-798f_{i+2}+482f_{i+3}-173f_{i+4}+27f_{i+5}}{1440}+E[f] \tag{34}$$

The order may be extended. Although these quadrature formulae contain negative weights they give good approximations up to order 6. In section 10 results are given using various orders.

8. THE OVERALL ALGORITHM

The method operates by checking first the normal co-ordinate truncation errors and then the streamwise errors. Equations (25) and (27) are solved repeatedly, with (26) being integrated before these are obtained. This is done because (25) is non-linear and is coupled to (26) and (27). Equation (25) is linearized with a Newton scheme.

All these equations contain a streamwise derivative term. These derivatives are replaced either by a high order implicit approximation or a linearized Crank–Nicolson scheme is used. When the Crank–Nicolson scheme is used the values of ϕ^* are determined at the points $((m+\theta)\delta x, i\delta\eta)$, $i=1,\ldots,n$ with $\theta=\frac{1}{2}$. The schemes in (31)–(34) are used to perform the normal co-ordinate integration in both cases.

9. ACCELERATING THE CONVERGENCE TO REDUCE THE TRUNCATION ERRORS

In this section a reliable way of implementing a truncation error reduction and of estimating the order of a difference approximation is presented. Let

$$x_i^{(0)} = x_i + 4^p a_i h^p, \quad x_i^{(1)} = x_i + 2^p a_i h^p \quad \text{and} \quad x_i^{(2)} = x_i + a_i h^p \tag{35}$$

where p is the order of the difference approximation and $x_i^{(0)}$ is the ith component of the dependent variable solved on a uniform mesh of interval size $4h$, $x_i^{(1)}$ that obtained on a $2h$ mesh and $x_i^{(2)}$ that on an h mesh. x_i is the exact solution (this is not strictly true, as x_i includes higher order truncation errors). The aim is to eliminate the leading term of the truncation error and estimate p. This may be

done by an Aitken δ^2 process:

$$y_i^* = x_i^{(2)} + s_i^*(x_i^{(2)} - x_i^{(1)}) \quad \text{with} \quad s_i^* = \frac{x_i^{(1)} - x_i^{(2)}}{x_i^{(0)} - 2x_i^{(1)} + x_i^{(2)}} \tag{36}$$

The main problem of applying this convergence acceleration is that the denominator for s_i^* may become very small. Jennings[5] has proposed the following scheme which circumvents the problem. [Whereas Jennings applied this scheme to matrix iterative processes (the power method for dominant eigenvalues and Jacobi iteration for linear systems) the above system is governed by a diagonal matrix. This is important, as the matrix must be symmetric for first difference modulation (see (39)) to always improve the approximation]:

$$\mathbf{y} = \mathbf{x}^{(2)} + s(\mathbf{x}^{(2)} - \mathbf{x}^{(1)}) \tag{37}$$

where $\mathbf{x}$ and $\mathbf{y}$ are vectors with a single scalar value of s which is given by

$$s = \frac{\mathbf{w}^{\mathrm{T}}(\mathbf{x}^{(1)} - \mathbf{x}^{(2)})}{\mathbf{w}^{\mathrm{T}}(\mathbf{x}^{(0)} - 2\mathbf{x}^{(1)} + \mathbf{x}^{(2)})} \tag{38}$$

The vector $\mathbf{w}$ is chosen as $\mathbf{w} = \mathbf{x}^{(0)} - \mathbf{x}^{(1)}$. This is called first difference modulation by Jennings. An alternative method of calculating s_i^* is

$$s_i^* = \frac{\lambda_i^*}{1 - \lambda_i^*}, \quad \text{where} \quad \lambda_i^* = \frac{x_i^{(1)} - x_i^{(2)}}{x_i^{(0)} - x_i^{(1)}} \tag{39}$$

This defines the rate of decay of the truncation errors. In (37) a single value of λ is defined as

$$s = \frac{\lambda}{1 - \lambda} \tag{40}$$

This allows p to be calculated as

$$p = \log_2\left(\frac{1}{\lambda}\right) \tag{41}$$

In order for the acceleration to always improve the solution the condition

$$-1 < \lambda_i^* < 1 \tag{42}$$

must be satisfied for all i. It was found that, in some cases, the inequalities in (42) were not satisfied near the edge of the boundary layer where the solution was relatively more accurate than near the wall. Accordingly the acceleration is only applied for the values of i for which (42) is satisfied for $1, 2, 3, \ldots i$. When applying this convergence acceleration to reduce the truncation errors in the normal co-ordinate direction the problem of finding an interpolating function to 'fill in the holes' was intractable. The calculation is of the stagnation point profile at which the equations become ordinary. The improved values are only defined on the mesh for which $\mathbf{x}^{(1)}$ has been calculated.

In Tables I and II the errors between the improved solution and the solution on a quartered mesh (compared to the finest mesh of the Jennings method) are compared with the errors of the point adjacent to them after interpolation. It can be seen that, whereas the error in the improved solution is well behaved, that in the interpolated solution is not. In all cases the error is the relative error.

The interpolating functions tried were a natural cubic spline and various orders of skew Lagrangian polynomial.

An alternative interpolating function is to fit the Lagrangian polynomial through the points f_i,

Table I. Results, near the wall, of interpolating in the stagnation point profile using a natural cubic spline

u_{error}	$u_{inter\cdot error}$	s_{error}	$s_{inter\cdot error}$
0	0·035	0	0·012
0·000045	0·057	0·000014	0·044
0·000033	0·0035	0·000016	0·0038
0·000012	0·024	0·000022	0·024
0·000015	0·0011	0·000040	0·00042
0·000039	0·016	0·000065	0·017
0·000049	0·0012	0·000080	0·00036
0·000042	0·013	0·000074	0·013
0·000028	0·0015	0·000053	0·000022
0·000015	0·012	0·000031	0·011
0·0000075	0·0014	0·000016	0·000049

Table II. Results, near the wall, of interpolating in the stagnation point profile using a skew Lagrangian polynomial with $p = 8$

u_{error}	$u_{inter\cdot error}$	s_{error}	$s_{inter\cdot error}$
0	0·00017	0	0·00011
0·000045	0·000032	0·000014	0·00015
0·000033	0·000090	0·000016	0·000038
0·000012	0·000049	0·000022	0·000053
0·000015	0·000036	0·000040	0·0000088
0·000039	0·000077	0·000065	0·000085
0·000049	0·000062	0·000080	0·00011
0·000042	0·000032	0·000074	0·000080
0·000028	0·000014	0·000053	0·000040
0·000015	0·0000069	0·000031	0·000016
0·0000075	0·0000044	0·000016	0·0000082

$f_{i+1}, f_{i+2}, \ldots, f_{i+p}$ and then evaluate this polynomial at $f_{i+1/2}$; this is the needed function value. Again the values of u and s beyond the edge of the boundary layer are 1. The value of p defines the order of the polynomial. This function gives much better interpolates than the natural cubic spline.

The maximum relative error between the $h/4$ mesh solution (without any acceleration) and the accelerated solution (which is only defined on the $2h$ mesh) is 0·000080. The maximum relative errors in the interpolated points (needed to give a solution on the other half of the points on the h mesh) are given in Table III.

From Table III it can be seen that all the errors in the interpolated points are considerably greater than those in the points directly computed from the acceleration. The skew Lagrangian polynomials are two orders of magnitude better than the spline, but increasing their order does not improve the interpolation.

For this reason the acceleration cannot be applied in the normal direction and the solution is computed and then recomputed with a halved normal step length; the maximum relative difference between these solutions then gives a bound on the errors.

Table III. Maximum relative errors in the interpolated points to 'fill in the holes' after Jennings acceleration

Interpolation function	Maximum relative error in u and s
Natural cubic spline	0·057
Skew Lagrange $p = 5$	0·00055
Skew Lagrange $p = 8$	0·00017
Skew Lagrange $p = 10$	0·00020
Skew Lagrange $p = 15$	0·00076

Finally it should be noted that the Jennings acceleration estimated the order of the normal approximation as 4·21, which is as expected, as the second derivatives have been replaced by a 4th order difference approximation and the first by a 5th order approximation.

The Crank–Nicolson method effectively approximates to streamwise derivatives by a central difference approximation and so is second order. The acceleration method can be applied in a streamwise direction, as there is no need for an interpolating function. However it seemed that investigating a third order fully implicit approximation may be useful. This is illustrated on Figure 2. The scheme is not self starting, and a Crank–Nicolson method must be used to calculate the first three sections.

The approximation

$$\frac{\partial f}{\partial x} = \frac{11f_i - 18f_{i-1} + 9f_{i-2} - 2f_{i-3}}{6\delta x} - \frac{f^{(iv)}(\delta x)^3}{4} + \cdots \tag{43}$$

replaces the streamwise first derivatives at x_i. This is also used (in the right hand side of (26)) to calculate values of ϕ^*. Whereas it is simple to apply the acceleration method when using the Crank–Nicolson scheme (the problem is solved with halved and then quartered step lengths) more care must be taken with the implicit scheme, so that the order is consistent.

The circled points (in Figure 3) show what sections are used in computing the streamwise derivatives. The sections with squares around them are computed with third order approximations. Because of this the 5 section scheme in steps 3, 4 and 5 is also third order.

In the scheme separation shows as a divergence in the non-linear iteration (this was noted by Cooke and Mangler[3]). A least squares straight line is fitted through the iteration differences (these are also taken as the maximum relative differences) and when the gradient becomes positive (after, say, 10 iterations have been performed) then the separation point is deemed to be in the interval between the previous streamwise section and the one being computed. The streamwise step length is then halved and an attempt made to recalculate the section. By limiting the number of times that this streamwise step bisection occurs the accuracy with which the separation point is calculated may be controlled.

10. RESULTS

All the runs were done for an asymptotic wedge as described in Appendix 2 of Reference 6, using the piston theory described in Appendix 1 of Reference 6 to give edge conditions. The edge velocities are shown in Figure 7. This was for a 3° semi-angle wedge at 10° incidence with a nose radius of 0·05 m. The solution is for the first 1 m of the underside of the wedge, which becomes flat

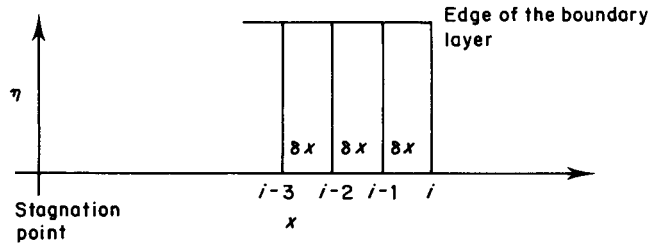

Figure 2. The implicit streamwise difference scheme

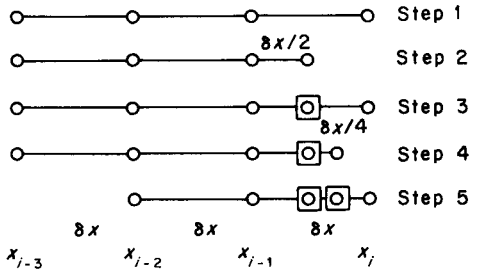

Figure 3. The implicit streamwise schemes for Jennings' acceleration

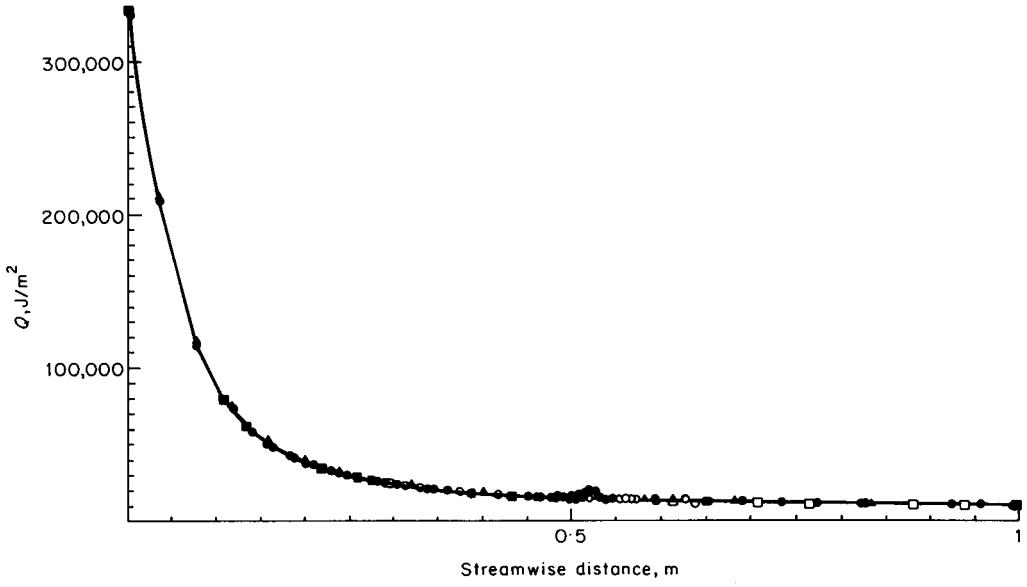

Figure 4. Crank–Nicolson with 3, 4, 5, 6 and 7 point ϕ^* formulae. The heat transfer (in J/m^2) are plotted against streamwise distance

0·5 m. from the nose. The maximum relative error tolerance is 0·005. The altitude was taken as 65 kilometres and, from Fiona MacDonald's report,[7] the free stream density was 0·000148375 kg/(m^3), the free stream temperature was 229·4 K and the free stream velocity was 5463 m/s, giving a Mach number of 18. An ideal gas was assumed with the gas constant $R = 287$. The specific heat ratio was 1·4 and the Prandtl number 0·72; the viscosity varies by Sutherland's law with Sutherland's constant being 117 K.

Equation (34) defines a 6 point quadrature formula for calculating values of the stream function ϕ^*. It seemed appropriate to see whether lower order formulae could be more efficient as they would involve fewer multiplications. Figure 4 shows the effect on the heat transfers when n used in the quadrature formula was taken as 3, 4, 5, 6 and 7. At the point at which the wedge becomes flat the 3 point formula displays an oscillation. These calculations were all done using a linearized Crank–Nicolson method.

Figure 5 shows the same range of quadrature orders when the 3rd order implicit method was used. The oscillation disappears.

Figure 6 shows a set of heat transfers from the Crank–Nicolson method plotted (as dots) on the heat transfers from the 3rd order implicit method plotted as a set of straight lines. A 9th order ϕ^* quadrature formula was used.

Figure 8 and 9 show the displacement and momentum thicknesses and the skin frictions, respectively. The lower line (for the first section) in Figure 8 is the displacement thickness. A negative displacement thickness is possible in highly compressible flows.

Figures 10 and 11 show an interesting feature of the normal co-ordinate stretching. The co-ordinate transformation was done primarily so that the increasing width of the boundary layer in the physical dimension could be mapped into a constant width in the transformed normal co-ordinate (if stagnation conditions are used as reference this is between 5 and 7). However, because of the compressibility effect the transform also makes the gradients in the transformed system much

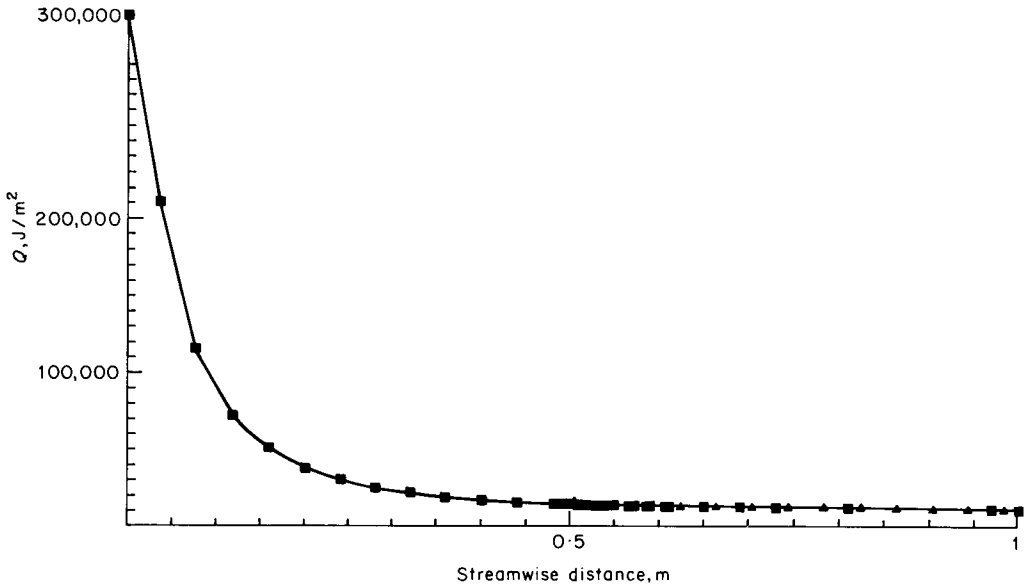

Figure 5. 3rd order implicit scheme with 3, 4, 5, 6 and 7 point ϕ^* formulae. The heat transfers (in J/m^2) are plotted against streamwise distance

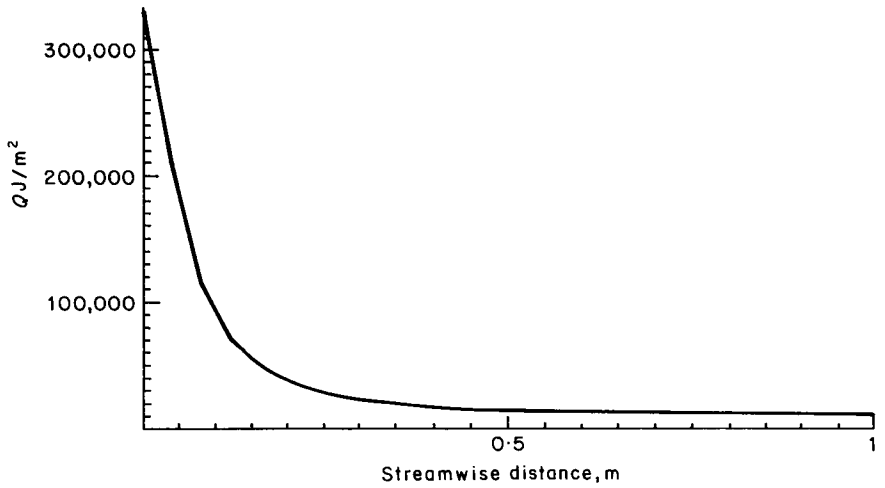

Figure 6. Comparison of Crank–Nicolson and 3rd order implicit schemes. The heat transfers (in J/m^2) are plotted against streamwise distance

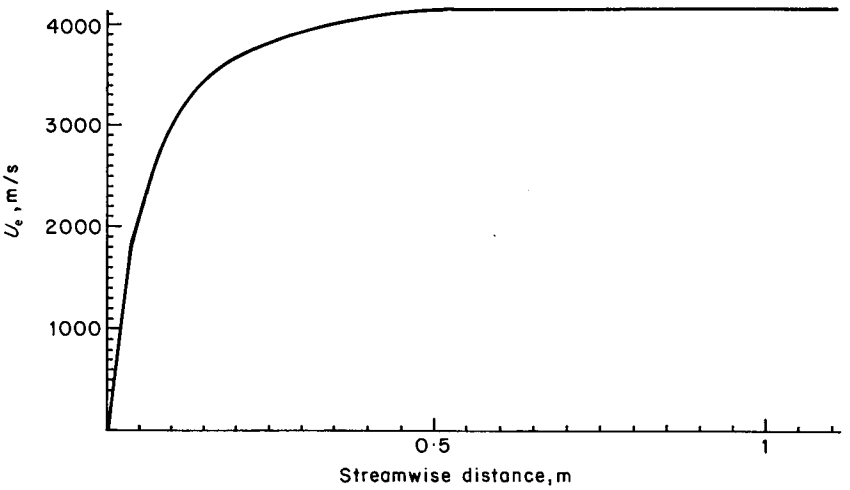

Figure 7. Edge velocities in m/s for the test problem

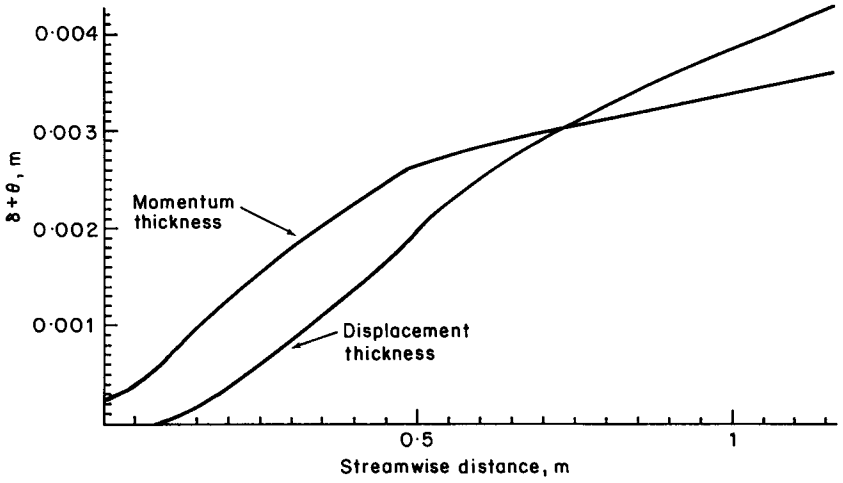

Figure 8. Displacement and momentum thicknesses in metres

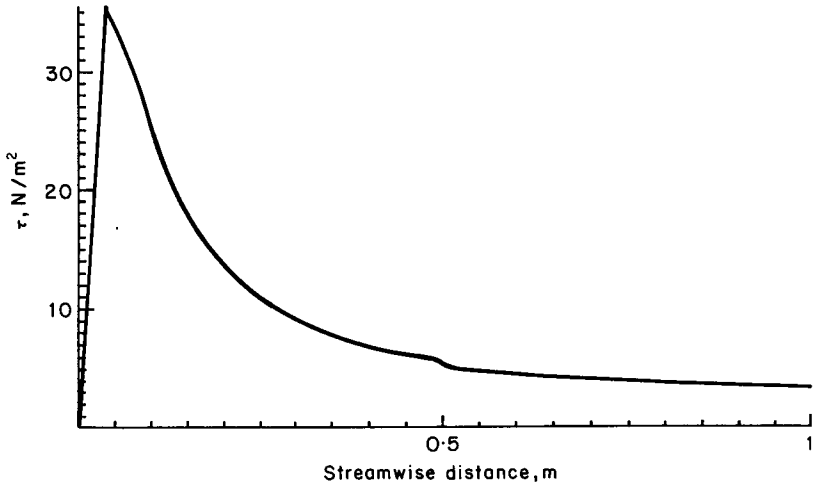

Figure 9. Skin friction in N/m^2

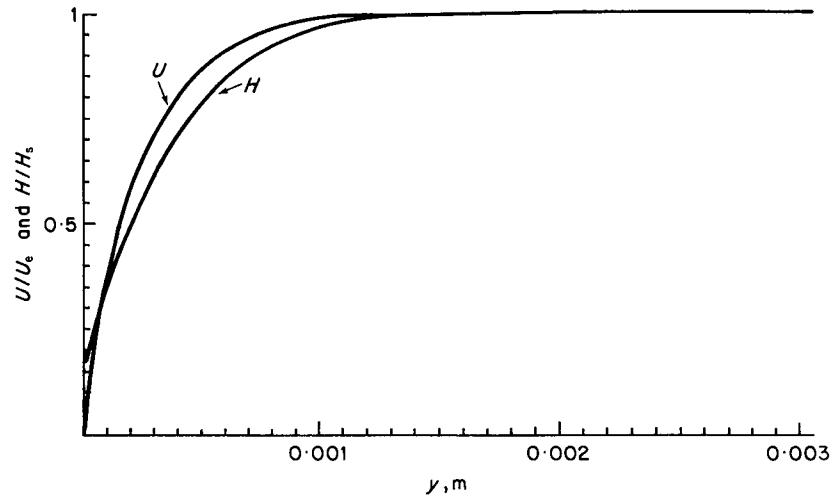

Figure 10. Stagnation point profile in the physical normal co-ordinate (m)

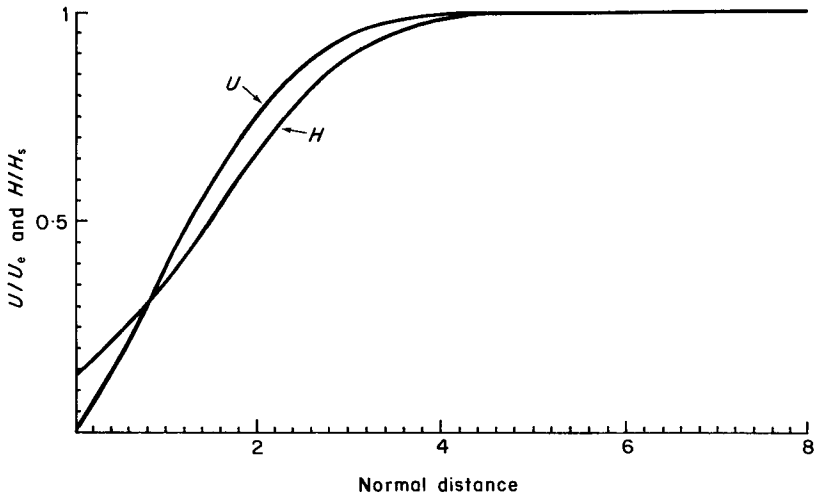

Figure 11. Stagnation point profile with the transformed normal co-ordinate η

Table IV. Times in minutes and seconds to solve the above problem to the specified accuracy

n_d	n_q	C–N without Jennings' acceleration	C–N with Jennings' acceleration	Implicit 3rd order without Jennings' acceleration	Implicit 3rd order with Jennings' acceleration
3	4	27:07	25:41	—	—
6	4	15:24	11:37	14:32	10:06
6	5	18:04	15:20	15:29	8:13
6	6	18:34	13:03	16:55	7:55
6	7	17:37	16:05	16:50	8:25

less severe than those in the physical one. Figure 10 shows a stagnation point profile in the physical co-ordinate system, whereas Figure 11 shows the profile in the transformed co-ordinate.

Results showing the times taken to solve above problem using various methods are given in Table IV. n_d is the number of points in the difference scheme (3—central difference, 6—skew scheme). n_q is the number of points in the quadrature formula. All the above computations were performed on a VAX 11/780.

11. CONCLUSIONS

The most rapid way of solving these equations is to use the high order scheme in the normal co-ordinate direction with the 3rd order implicit scheme in the streamwise direction coupled with the acceleration method. There would not appear to be any reason to use a more than 5 point quadrature formula for calculating ϕ^*. Jennings' acceleration (applied only in the streamwise direction) always allowed the flow to be calculated more rapidly. The reason why Jennings shows a much more marked improvement for the implicit scheme rather than Crank–Nicolson is that the implicit scheme is 3rd order and requires 5 checked normal sections to be calculated for a single step (see Figure 3), whereas the Crank–Nicolson scheme is 2nd order and requires 7 checked normal sections to be calculated.

The methods all adaptively altered both their normal and streamwise step lengths to attempt to meet the relative error bound as closely as possible. This is essential if problems with very high gradients in their edge velocities are to be solved reasonably efficiently.

ACKNOWLEDGEMENTS

I am indebted to Professor T. R. F. Nonweiler for helping me to start work on this problem and to Claire for being herself.

REFERENCES

1. K. Stewartson, *The Theory of Laminar Boundary Layers in Compressible Fluids*, Oxford Mathematical Monographs, 1964.
2. N. A. Jaffe and A. M. O. Smith, 'Calculation of laminar boundary layers by means of a differential-difference method', in D. Kuchemann (ed.), *Progress in Aerospace Sciences Vol. 12*, Pergamon Press, 1972.
3. J. C. Cooke and K. W. Mangler, 'The numerical solution of the laminar boundary layer equations for an ideal gas in two

and three dimensions', *A.G.A.R.D. (Nato Advisory group on aircraft research and development) conference (revised) on Numerical solution of viscous flows no. 60*, 1970, pp. 45–50.

4. D. W. Clutter and A. M. O. Smith, Solution of the General Boundary-layer Equations for Compressible Laminar Flow Including Transverse Curvature', *Douglas Aircraft Co. Report No. LB-31088* February 1963 (Revised October 1984).
5. Alan Jennings, 'Accelerating the convergence of matrix iterative processes', *Journal of the Institute of Mathematics and its Applications* 99–110 (1971).
6. R. G. Friel, 'Numerical methods in the analysis of caret wings', *Ph.D. Thesis*, Trinity College, University of Dublin, January 1983.
7. Fiona MacDonald, 'The relationship between the initial Mach number at the start of a non-oscillatory glide and the range for a wave rider type lift producing re-entry vehicle', *Internal report*, Department of Aeronautics and Fluid Mechanics. Glasgow University, 1973.